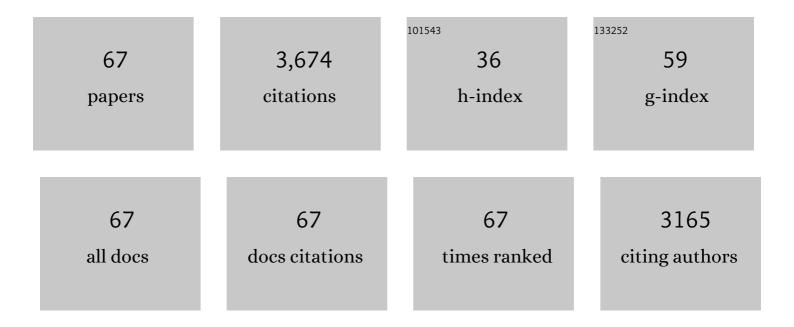
Youwen Yang

List of Publications by Year in descending order

Source: https://exaly.com/author-pdf/10778071/publications.pdf Version: 2024-02-01



#	Article	IF	CITATIONS
1	Semicoherent strengthens graphene/zinc scaffolds. Materials Today Nano, 2022, 17, 100163.	4.6	18
2	Additive manufacturing of Bio-inspired ceramic bone Scaffolds: Structural Design, mechanical properties and biocompatibility. Materials and Design, 2022, 217, 110610.	7.0	53
3	Mechanical properties and biocompatibility of MgO / Ca3(PO4)2 composite ceramic scaffold with high MgO content based on digital light processing. Ceramics International, 2022, 48, 21175-21186.	4.8	11
4	Fabrication of a zirconia/calcium silicate composite scaffold based on digital light processing. Ceramics International, 2022, 48, 25923-25932.	4.8	12
5	Trabecular-like Ti–6Al–4V scaffold for bone repair: A diversified mechanical stimulation environment for bone regeneration. Composites Part B: Engineering, 2022, 241, 110057.	12.0	38
6	Dilemmas and countermeasures of Fe-based biomaterials for next-generation bone implants. Journal of Materials Research and Technology, 2022, 20, 2034-2050.	5.8	9
7	Dual alloying improves the corrosion resistance of biodegradable Mg alloys prepared by selective laser melting. Journal of Magnesium and Alloys, 2021, 9, 305-316.	11.9	45
8	Fabrication and properties of CaSiO3/ Sr3(PO4)2 composite scaffold based on extrusion deposition. Ceramics International, 2021, 47, 4783-4792.	4.8	16
9	Microstructure evolution and texture tailoring of reduced graphene oxide reinforced Zn scaffold. Bioactive Materials, 2021, 6, 1230-1241.	15.6	132
10	Layer-dependent photocatalysts of GaN/SiC-based multilayer van der Waals heterojunctions for hydrogen evolution. Catalysis Science and Technology, 2021, 11, 3059-3069.	4.1	21
11	A novel design of SiH/CeO ₂ (111) van der Waals type-II heterojunction for water splitting. Physical Chemistry Chemical Physics, 2021, 23, 2812-2818.	2.8	49
12	Boosting the photocatalytic hydrogen evolution performance of monolayer C ₂ N coupled with MoSi ₂ N ₄ : density-functional theory calculations. Physical Chemistry Chemical Physics, 2021, 23, 8318-8325.	2.8	49
13	Design and Compressive Fatigue Properties of Irregular Porous Scaffolds for Orthopedics Fabricated Using Selective Laser Melting. ACS Biomaterials Science and Engineering, 2021, 7, 1663-1672.	5.2	17
14	A bifunctional bone scaffold combines osteogenesis and antibacterial activity via in situ grown hydroxyapatite and silver nanoparticles. Bio-Design and Manufacturing, 2021, 4, 452-468.	7.7	48
15	Rare earth improves strength and creep resistance of additively manufactured Zn implants. Composites Part B: Engineering, 2021, 216, 108882.	12.0	66
16	Core–shell-Structured ZIF-8@PDA-HA with Controllable Zinc Ion Release and Superior Bioactivity for Improving a Poly- <scp>I</scp> -lactic Acid Scaffold. ACS Sustainable Chemistry and Engineering, 2021, 9, 1814-1825.	6.7	50
17	Laser-Sintered Mg-Zn Supersaturated Solid Solution with High Corrosion Resistance. Micromachines, 2021, 12, 1368.	2.9	7
18	Laser Additive Manufacturing of Zinc Targeting for Biomedical Application. International Journal of Bioprinting, 2021, 8, 501.	3.4	15

#	Article	IF	CITATIONS
19	Functionalized BaTiO3 enhances piezoelectric effect towards cell response of bone scaffold. Colloids and Surfaces B: Biointerfaces, 2020, 185, 110587.	5.0	102
20	Mg bone implant: Features, developments and perspectives. Materials and Design, 2020, 185, 108259.	7.0	251
21	A magnetic micro-environment in scaffolds for stimulating bone regeneration. Materials and Design, 2020, 185, 108275.	7.0	101
22	Fabrication and properties of zirconia/hydroxyapatite composite scaffold based on digital light processing. Ceramics International, 2020, 46, 2300-2308.	4.8	96
23	Selective laser melted Fe-Mn bone scaffold: microstructure, corrosion behavior and cell response. Materials Research Express, 2020, 7, 015404.	1.6	50
24	Surface modification enhances interfacial bonding in PLLA/MgO bone scaffold. Materials Science and Engineering C, 2020, 108, 110486.	7.3	46
25	Electrostatic self-assembly of pFe3O4 nanoparticles on graphene oxide: A co-dispersed nanosystem reinforces PLLA scaffolds. Journal of Advanced Research, 2020, 24, 191-203.	9.5	58
26	A peritectic phase refines the microstructure and enhances Zn implants. Journal of Materials Research and Technology, 2020, 9, 2623-2634.	5.8	30
27	Graphene-assisted barium titanate improves piezoelectric performance of biopolymer scaffold. Materials Science and Engineering C, 2020, 116, 111195.	7.3	26
28	Graphene oxide assists polyvinylidene fluoride scaffold to reconstruct electrical microenvironment of bone tissue. Materials and Design, 2020, 190, 108564.	7.0	81
29	Mesoporous Carbon as Galvanic-Corrosion Activator Accelerates Fe Degradation. Applied Sciences (Switzerland), 2020, 10, 2487.	2.5	2
30	Magnetically actuated bone scaffold: Microstructure, cell response and osteogenesis. Composites Part B: Engineering, 2020, 192, 107986.	12.0	67
31	Laser additive manufacturing of Mg-based composite with improved degradation behaviour. Virtual and Physical Prototyping, 2020, 15, 278-293.	10.4	82
32	A strawberry-like Ag-decorated barium titanate enhances piezoelectric and antibacterial activities of polymer scaffold. Nano Energy, 2020, 74, 104825.	16.0	264
33	MnO2 catalysis of oxygen reduction to accelerate the degradation of Fe-C composites for biomedical applications. Corrosion Science, 2020, 170, 108679.	6.6	31
34	Metal organic frameworks as a compatible reinforcement in a biopolymer bone scaffold. Materials Chemistry Frontiers, 2020, 4, 973-984.	5.9	67
35	Construction of an electric microenvironment in piezoelectric scaffolds fabricated by selective laser sintering. Ceramics International, 2019, 45, 20234-20242.	4.8	11
36	Strong corrosion induced by carbon nanotubes to accelerate Fe biodegradation. Materials Science and Engineering C, 2019, 104, 109935.	7.3	18

#	Article	IF	CITATIONS
37	Bioceramic enhances the degradation and bioactivity of iron bone implant. Materials Research Express, 2019, 6, 115401.	1.6	13
38	Mechanical Properties of In-Situ Synthesis of Ti-Ti3Al Metal Composite Prepared by Selective Laser Melting. Metals, 2019, 9, 1121.	2.3	5
39	Trabecular-like Ti-6Al-4V scaffolds for orthopedic: fabrication by selective laser melting and in vitro biocompatibility. Journal of Materials Science and Technology, 2019, 35, 1284-1297.	10.7	149
40	Laser additive manufacturing of Zn-2Al part for bone repair: Formability, microstructure and properties. Journal of Alloys and Compounds, 2019, 798, 606-615.	5.5	93
41	nMgO-incorporated PLLA bone scaffolds: Enhanced crystallinity and neutralized acidic products. Materials and Design, 2019, 174, 107801.	7.0	58
42	Montmorillonite with unique interlayer space imparted polymer scaffolds with sustained release of Ag+. Ceramics International, 2019, 45, 11517-11526.	4.8	11
43	Uniform degradation mode and enhanced degradation resistance of Mg alloy via a long period stacking ordered phase in the grain interior. Materials Research Express, 2019, 6, 065406.	1.6	3
44	Crystallinity and Reinforcement in Poly-L-Lactic Acid Scaffold Induced by Carbon Nanotubes. Advances in Polymer Technology, 2019, 2019, 1-10.	1.7	12
45	3D honeycomb nanostructure-encapsulated magnesium alloys with superior corrosion resistance and mechanical properties. Composites Part B: Engineering, 2019, 162, 611-620.	12.0	124
46	A continuous net-like eutectic structure enhances the corrosion resistance of Mg alloys. International Journal of Bioprinting, 2019, 5, 207.	3.4	15
47	Graphene Oxide Induces Ester Bonds Hydrolysis of Poly-l-lactic Acid Scaffold to Accelerate Degradation. International Journal of Bioprinting, 2019, 6, 249.	3.4	32
48	Hydrolytic Expansion Induces Corrosion Propagation for Increased Fe Biodegradation. International Journal of Bioprinting, 2019, 6, 248.	3.4	3
49	Regulating Degradation Behavior by Incorporating Mesoporous Silica for Mg Bone Implants. ACS Biomaterials Science and Engineering, 2018, 4, 1046-1054.	5.2	67
50	Selective laser melting of Zn–Ag alloys for bone repair: microstructure, mechanical properties and degradation behaviour. Virtual and Physical Prototyping, 2018, 13, 146-154.	10.4	49
51	A Multimaterial Scaffold With Tunable Properties: Toward Bone Tissue Repair. Advanced Science, 2018, 5, 1700817.	11.2	264
52	A combined strategy to enhance the properties of Zn by laser rapid solidification and laser alloying. Journal of the Mechanical Behavior of Biomedical Materials, 2018, 82, 51-60.	3.1	103
53	Biodegradation mechanisms of selective laser-melted Mg– <i>x</i> Al–Zn alloy: grain size and intermetallic phase. Virtual and Physical Prototyping, 2018, 13, 59-69.	10.4	30
54	Lanthanum-Containing Magnesium Alloy with Antitumor Function Based on Increased Reactive Oxygen Species. Applied Sciences (Switzerland), 2018, 8, 2109.	2.5	14

#	Article	IF	CITATIONS
55	Ag-Introduced Antibacterial Ability and Corrosion Resistance for Bio-Mg Alloys. BioMed Research International, 2018, 2018, 1-13.	1.9	16
56	Wrapping effect of secondary phases on the grains: increased corrosion resistance of Mg–Al alloys. Virtual and Physical Prototyping, 2018, 13, 292-300.	10.4	17
57	An nMgO containing scaffold: Antibacterial activity, degradation properties and cell responses. International Journal of Bioprinting, 2018, 4, 120.	3.4	20
58	Mechanism for corrosion protection of \hat{I}^2 -TCP reinforced ZK60 via laser rapid solidification. International Journal of Bioprinting, 2018, 4, 124.	3.4	13
59	Additive manufacturing of bone scaffolds. International Journal of Bioprinting, 2018, 5, 148.	3.4	120
60	A multi-scale porous scaffold fabricated by a combined additive manufacturing and chemical etching process for bone tissue engineering. International Journal of Bioprinting, 2018, 4, 133.	3.4	2
61	Graphene oxide as an interface phase between polyetheretherketone and hydroxyapatite for tissue engineering scaffolds. Scientific Reports, 2017, 7, 46604.	3.3	73
62	Laser rapid solidification improves corrosion behavior of Mg-Zn-Zr alloy. Journal of Alloys and Compounds, 2017, 691, 961-969.	5.5	104
63	Microstructure Evolution and Biodegradation Behavior of Laser Rapid Solidified Mg–Al–Zn Alloy. Metals, 2017, 7, 105.	2.3	37
64	Rare Earth Element Yttrium Modified Mg-Al-Zn Alloy: Microstructure, Degradation Properties and Hardness. Materials, 2017, 10, 477.	2.9	37
65	The Enhancement of Mg Corrosion Resistance by Alloying Mn and Laser-Melting. Materials, 2016, 9, 216.	2.9	48
66	The microstructure, mechanical properties and degradation behavior of laser-melted Mg Sn alloys. Journal of Alloys and Compounds, 2016, 687, 109-114.	5.5	42
67	System development, formability quality and microstructure evolution of selective laser-melted magnesium. Virtual and Physical Prototyping, 2016, 11, 173-181.	10.4	61